JOURNAL OF VIROLOGY, Feb. 2007, p. 1714–1726 Vol. 81, No. 4
0022-538X/07/$08.00+0 doi:10.1128/JVI.01863-06

Hepatitis B Virus X Protein Induces Perinuclear Mitochondrial Clustering in Microtubule- and Dynein-Dependent Manners▽

Sujeong Kim,[1] Hye-Young Kim,[2] Seungmin Lee,[1] Sung Woo Kim,[3] Seonghyang Sohn,[4] Kyongmin Kim,[2]* and Hyeseong Cho[1]*

Department of Biochemistry,[1] and Department of Microbiology,[2] Ajou University School of Medicine, Suwon, Korea; Animal Biotechnology Division, National Livestock Research Institute, Suwon, Korea[3]; and Laboratory of Cell Biology, Ajou University Institute for Medical Sciences, Suwon, Korea[4]

Received 26 August 2006/Accepted 27 November 2006

The hepatitis B virus (HBV) X protein (HBx) is thought to play a key role in HBV replication and the development of liver cancer. It became apparent that HBx induces mitochondrial clustering at the nuclear periphery, but the molecular basis for mitochondrial clustering is not understood. Since mitochondria move along the cytoskeleton as a cargo of motor proteins, we hypothesized that mitochondrial clustering induced by HBx occurs by an altered intracellular motility. Here, we demonstrated that the treatment of HBx-expressing cells with a microtubule-disrupting drug (nocodazole) abrogated mitochondrial clustering, while the removal of nocodazole restored clustering within 30 to 60 min, indicating that mitochondrial transport is occurring in a microtubule-dependent manner. The addition of a cytochalasin D-disrupting actin filament, however, did not measurably affect mitochondrial clustering. Mitochondrial clustering was further studied by observations of HBV-related hepatoma cells and HBV-replicating cells. Importantly, the abrogation of the dynein activity in HBx-expressing cells by microinjection of a neutralizing anti-dynein intermediate-chain antibody, dynamitin overexpression, or the addition of a dynein ATPase inhibitor significantly suppressed the mitochondrial clustering. In addition, HBx induced the activation of the p38 mitogen-activated protein kinase (MAPK) and inhibition of the p38 kinase activity by SB203580-attenuated HBx-induced mitochondrial clustering. Taken together, HBx activation of the p38 MAPK contributed to the increase in the microtubule-dependent dynein activity. The data suggest that HBx plays a novel regulatory role in subcellular transport systems, perhaps facilitating the process of maturation and/or assembly of progeny particles during HBV replication. Furthermore, mitochondrion aggregation induced by HBx may represent a cellular process that underlies disease progression during chronic viral infection.

Human hepatitis B virus (HBV) (family *Hepadnaviridae*) shows such a strong liver pathogenicity that it is estimated that there are over 350 million chronic human carriers of HBV worldwide. HBV infection causes acute and chronic hepatitis, which can further progress to cirrhosis and hepatocellular carcinoma (6, 29). Although epidemiological evidence strongly supports the importance of chronic HBV infection as a major etiological factor for the development of hepatocellular carcinoma, its molecular mechanism of pathogenesis and carcinogenesis remains to be clearly understood. The human hepatitis B virus X (HBx) protein (154 amino acids) is encoded by the HBV genome and has drawn a great deal of attention for its pleiotropic activities in cells (3, 34). HBx was initially identified as a viral transcriptional transactivator. HBx does not directly bind DNA but activates a wide range of viral and cellular regulatory elements (37, 41). HBx in the nucleus can increase the transcriptional activity by interactions with nuclear transcription factors or with the basal transcriptional machinery of host RNA polymerases (9, 27, 28, 32). It was shown that at low levels of expression, HBx is localized primarily in the nucleus (16). Besides its nuclear function, HBx in the cytoplasm participates in a wide variety of cellular signal transduction pathways. In fact, HBx was found to be localized predominantly in the cytoplasm of livers in patient infected with HBV and most cultured cells (11, 17, 20). HBx activates multiple cytoplasmic signaling pathways such as Ras-Raf-mitogen-activated protein kinase (MAPK), phosphoinositide 3-kinase, Src kinase, and Wnt/β-catenin signaling (5, 8, 12, 23, 26), which can contribute to increases in oncogenic risks for HBV-infected livers. In addition, cytoplasmic HBx can enhance HBV replication by triggering cytosolic calcium release from mitochondria, which in turn activates proline-rich tyrosine kinase 2 (Pyk2) and Src kinase (4, 5). All these reports along with several other studies support a pivotal role of HBx in liver disease pathogenesis and carcinogenesis.

Using both immunofluorescence microscopy and subcellular fractionation techniques, HBx has been shown to substantially associate with mitochondria (16, 35, 39). HBx can interact directly with an outer mitochondrial voltage-dependent anion channel, VDAC3 (33). The mitochondrial association of HBx caused an alteration of mitochondrial membrane potential and increased intracellular reactive oxygen species (ROS) levels (35, 42). Depending on the severity of mitochondrial dysfunction, HBx may either cause apoptotic cell death or subject cells to oxidative stress mediated through the down-regulation of mitochondrial enzymes involved in oxidative phosphorylation (25) or by the activation of NF-κB and STAT3 (42). Thus, the mitochondrion-associated HBx contributes to pathophysiolog-

* Corresponding author. Mailing address: Department of Biochemistry, Ajou University School of Medicine, 5 Wonchon-dong, Yeongtong-gu, Suwon 443-721, Korea. Phone: 82-31-219-5052. Fax: 82-31-219-5059. E-mail: hscho@ajou.ac.kr.

▽ Published ahead of print on 6 December 2006.

ical changes of liver cells imposing continuous oxidative stress during chronic HBV infection. Intriguingly, the mitochondrial association of HBx often accompanies abnormal mitochondrial aggregation near the nucleus, especially in cells with high levels of HBx expression (16, 35, 39). It is not known whether abnormal mitochondrial aggregation is linked to the functional alteration of mitochondria, but it was suggested to be a consequence of mitochondrial damage or apoptosis (25, 35, 39). However, we reasoned that since mitochondria move along the cytoskeleton as a cargo of motor proteins (43), the observed mitochondrial clustering could instead result from an altered transport system in HBx-expressing cells.

Here, we used Chang and Huh7 cells expressing the HBx gene or the HBV genome to study a possible link between HBx and the regulation of the cellular transport system. We found that the expression of the HBx gene induces a microtubule-dependent perinuclear clustering of mitochondria. Furthermore, the functional blockage of dynein and the p38 MAPK in HBx-expressing cells significantly suppressed this mitochondrial movement. This is the first indication that the HBx viral protein possesses an intrinsic property to modulate intracellular motility.

MATERIALS AND METHODS

Materials. The rabbit anti-pericentrin antibody was kindly provided by Gordon K. Chan (University of Alberta, Canada). MitoTrackerRed and 4′,6-diamidine-2-phenylindole (DAPI) were obtained from Molecular Probes (Eugene, OR). Nocodazole, cytochalasin D, wortmannin, SB203580, calphostin C, and neutralizing anti-dynein intermediate-chain (clone 70.1) antibodies were obtained from Sigma (St. Louis, MO). Erythro-9-(2-hydroxy-3-nonyl)adenine (EHNA) was obtained from Calbiochem (Darmstadt, Germany), and the anti-phospho-extracellular signal-regulated kinase (ERK), anti-total ERK, and anti-phospho-p38 antibodies were obtained from Cell Signaling. For the detection of the HBx protein in immunofluorescence staining and Western blotting, a polyclonal rabbit anti-HBx antibody against a synthetic HBx peptide corresponding to residues 144 to 154, which was conjugated to keyhole limpet hemocyanin for immunization, was made (Lab Frontier, Seoul, Korea). The anti-hemagglutinin and anti-total-p38 antibodies were purchased from Santa Cruz (Santa Cruz, CA). The polyethylenimine (PEI) used for DNA transfection was purchased from Polysciences (Warrington, PA).

Plasmids. The pHBV 1.2-mer replicon and HBx-negative HBV were generously provided by Wang-Shick Ryu (Yonsei University, Korea). The HBx-negative HBV replicon contains a stop codon following the first and second AUG of the HBx gene. pPB was originally derived from HBV subtype adw R9, 1.3-mer of the HBV genome (2) and subcloned into pcDNA3 (Invitrogen) to express HBV under the cytomegalovirus immediate-early promoter (21). The cDNA expression vectors encoding dynamitin, p50 (1), mitogen-activated protein kinase kinase 6 (MKK6), and the active mutant of Raf-1 (Raf-CA) were kindly provided by Richard Vallee (Columbia University, NY), Aree Moon (Duksung Women's University, Seoul, Korea), and Kang-Yell Choi (Yonsei University, Seoul, Korea), respectively. The pEGFP expression vector was purchased from Clontech.

Cell lines. HBx-transfected ChangX-31 and ChangX-34 cells (45, 46) and parental Chang cells (CCL-13; ATCC), vector-transfected ChangV9 cells, and human hepatoma Huh7 cells were maintained in Dulbecco's modified Eagle's medium (DMEM) supplemented with 10% fetal bovine serum. Huh7-HBV cell lines were established by stably transfecting the pPB vector and carrying out antibiotic selection after challenge with 1 mg/ml of G418. SNU series of hepatoma cell lines were purchased from the Korean Cell Line Bank (Seoul, Korea).

Fluorescence and confocal microscopy. Cells were seeded directly onto coverslips and incubated overnight before being treated with or without 3.3 μM nocodazole for 2 h, as indicated. The nocodazole was removed by repeated washes with phosphate-buffered saline (PBS), and cells were stained for 30 min with 62 nM MitoTrackerRed. To detect the stable dynein complex in cells, cells were first permeabilized with 0.075% Triton X-100 containing PHEM buffer {12.5 mM HEPES, 30 mM PIPES [piperazine-*N*,*N*-bis(2-ethanesulfonic acid)], 5 mM EGTA, 2 mM $MgCl_2$, pH 7.4} for 5 min, followed by fixation with a methanol-acetone (1:1) solution, and the distribution of the dynein intermediate chain (DIC), a component of the dynein complex, was determined. Otherwise, samples were first fixed with a mixture of methanol-acetone and permeabilized with PHEM buffer containing 0.075% Triton X-100. Fixed cells were preincubated in blocking solution (1% bovine serum albumin in PBS) and then incubated with the appropriate primary antibodies (anti-α-tubulin, anti-β-actin, or anti-pericentrin) at 4°C. After overnight incubation, the cells were washed, probed with a fluorescence-conjugated secondary antibody in the presence of DAPI, and mounted for microscopy. Fluorescence images were acquired by fluorescence microscopy (Bx60; Olympus Optical) or confocal microscopy (LSM510; Zeiss). Approximately 20 to 40 mitochondria were present in a field observed with a ×40 objective.

Analysis of mitochondrial clustering. Mitochondrial clustering was judged by two criteria. When the area occupied by mitochondria in a cell was less than 40%, crescent-shaped or ring-shaped mitochondrial staining was observed (see Fig. 2 and 3). A manifest mitochondrial aggregation was used as the first criterion, and the analysis was carried out blind by two persons. For the second criterion of amorphous mitochondrial aggregation, the area occupied by mitochondria in a cell was outlined, automatically calculated using LSM5 Image Browser (Zeiss), and compared to the area of a whole cell. For convenience, the nuclear area was always included for the calculation, as shown in Fig. 4A. When the line was drawn, the mitochondria on the tubular network were included, whereas the small and scattered mitochondria in a distance were ignored. Each time, 10 to 20 different cells transfected with appropriate expression vectors along with pEGFP were used in two to four separate experiments. For the signaling inhibitor experiment shown in Fig. 6B, digital images of five different fields of the slide were analyzed by two persons in three separate experiments. When the percentage of mitochondrial area per cell was less than 60%, it was counted as mitochondrion-aggregated cells, whereas when the percentages were higher than 75%, those cells were considered to be cells with nonaggregated mitochondria.

Southern blotting. To analyze HBV DNA synthesis, core particles were isolated from Huh7-HBV cells as previously described (21). Briefly, cells were lysed and incubated overnight at 37°C with 20 U DNase I and 60 U micrococcal nuclease (Calbiochem). Cytoplasmic core particles were precipitated with 6.5% polyethylene glycol. Core DNA was extracted, separated by agarose gel electrophoresis, and hybridized to a ^{32}P-labeled random-primed probe specific for the HBV sequence.

Microinjection. ChangX-34 cells were seeded onto coverslips 24 h prior to microinjection and transferred into serum-free DMEM 2 h before microinjection. A neutralizing antibody against dynein intermediate chain and control mouse immunoglobulin G (IgG) were concentrated in a concentrator (Vivascience, Hanover, Germany) at 15,000 × *g* for 10 min, and 10 mg/ml dynein intermediate chain or 20 mg/ml mouse control IgG was then mixed with 20 mg/ml green fluorescent protein and diluted to a final concentration of 1 mg/ml. The resulting antibody mixtures were microinjected into ~300 cells on the stage of an Axiovert 100 apparatus (Zeiss, Germany) equipped with a micromanipulator (model 5171; Eppendorf, Germany) and an automatic micromanipulator (model 5246; Eppendorf). Four hours later, cells were treated with 3.3 μM nocodazole, washed, stained with MitoTrackerRed, and examined by confocal microscopy (Zeiss) for subcellular localization of mitochondria. Digital images of 50 to 100 individual mitochondria were obtained and analyzed according to the criteria of mitochondrial clustering.

Transfection. Chang or Huh7 cells were seeded onto coverslips in 60-mm dishes, incubated for 24 h, and then transfected with the appropriate expression vectors (pMyc-HBx, dynamitin, MKK6, or Raf-CA along with pEGFP as a transfection indicator) using PEI (Polysciences, Inc.). Briefly, 4 μg of DNA and 8 μl of PEI (1 mg/ml) were mixed into 200 μl of Opti-MEM (GibcoBRL, Life Technology), incubated for 10 min, and directly added to the culture dishes. After incubation overnight, any remaining extracellular DNA precipitates were removed by several washes with serum-free DMEM, and protein expression was allowed to occur for 12 to 48 h. The subcellular localization of mitochondria was then analyzed by MitoTrackerRed staining and observed by fluorescence or confocal microscopy.

RESULTS

The microtubule network is required for HBx-induced mitochondrial clustering. Mitochondrial aggregation accompanied by mitochondrial dysfunction and/or cell death has been found in cells expressing the HBx protein (25, 35, 39). However, no previous study has examined the mechanism by which HBx induces mitochondrial aggregation. Mammalian cells can have thousands

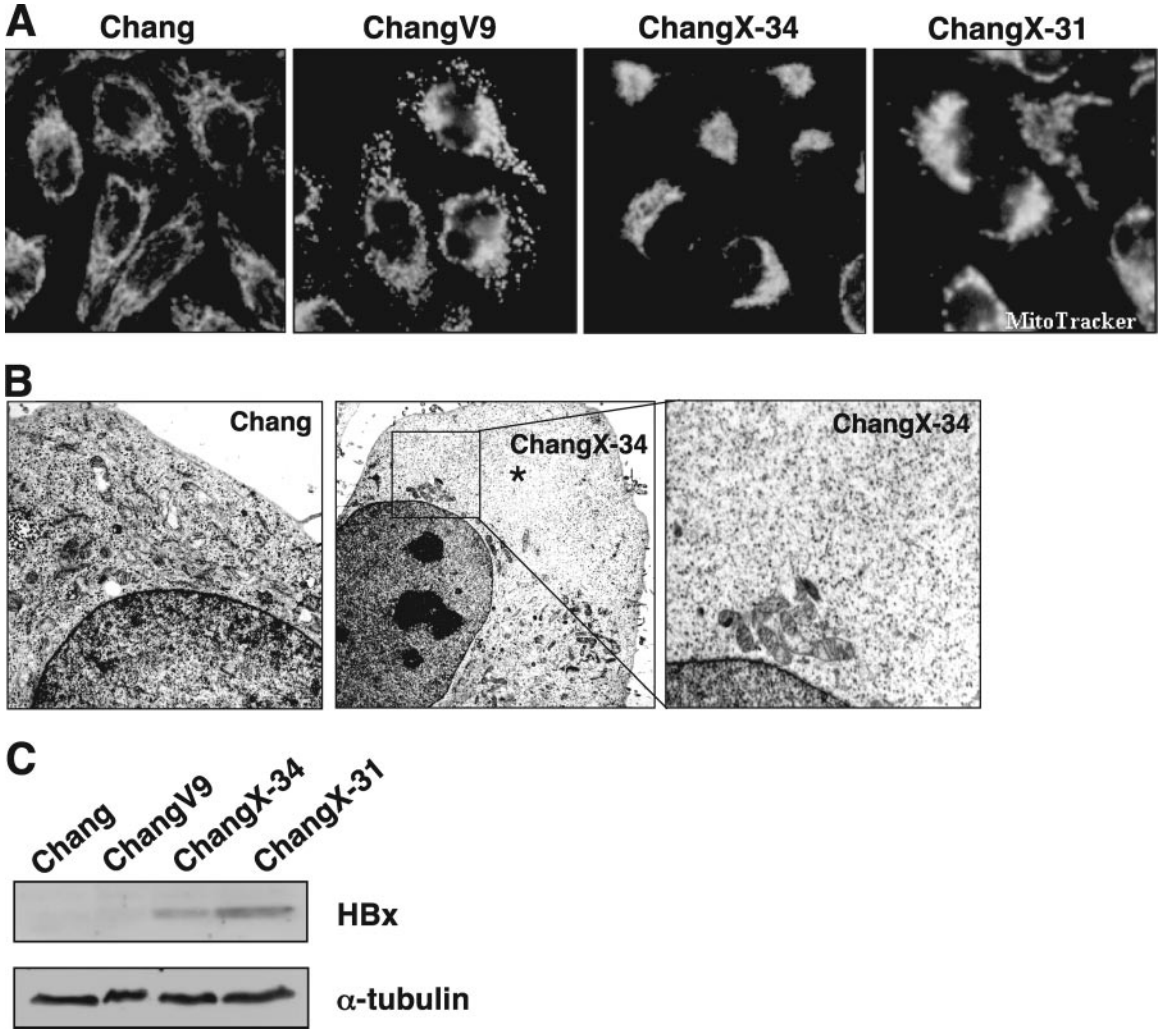

FIG. 1. HBx induces perinuclear clustering of mitochondria in HBx-expressing Chang cells. (A) Parental Chang, control vector-transfected ChangV9, and HBx-expressing ChangX-31 and ChangX-34 cells were incubated for 30 min with MitoTrackerRed. Cells were fixed with cold methanol-acetone (1:1) and examined for subcellular mitochondrial distribution under a fluorescence microscope. The microscopic pictures are representative of six independent experiments. The crescent pattern of mitochondrion distribution was used as a criterion to judge mitochondrial clustering. (B) Electron microscopic view of subcellular organelles in Chang and ChangX-34 cells. Asterisks mark areas that are free of organelles. The right panel shows an enlargement of the inset. (C) Expression levels of the HBx protein were determined by Western blotting using rabbit anti-HBx antibody. α-Tubulin levels were used as a loading control in each lane.

of mitochondria, which move along the cytoskeleton as a cargo of motor proteins. We hypothesized that mitochondrial clustering induced by HBx could occur by an altered intracellular motility. Here, we attempted to examine this hypothesis by utilizing Chang cell lines expressing the HBx gene (45, 46). As shown previously by others using Huh7 and HepG2 cells (25, 35, 39), we observed crescent-shaped mitochondrial aggregations (Fig. 1A) in HBx-expressing cells stained with the mitochondrion-specific fluorescent dye MitoTrackerRed. Virtually 80 to 90% of HBx-expressing cells showed distinct perinuclear mitochondrial clustering. In contrast, the mitochondria in the parental Chang cells and vector-transfected ChangV9 cells showed a typical cytoplasmic spreading pattern. Electron microscopy revealed that the mitochondrial aggregation in ChangX-34 cells was often concentrated around the nuclear periphery (Fig. 1B, middle and right, magnification of the inset), whereas these organelles were homogenously distributed in the cytoplasm of control Chang cells (Fig. 1B, left). Notably, the nonperiplasmic areas of HBx-expressing cells were almost free of mitochondria (Fig. 1B, middle, asterisks). Unlike the previous notion that cells with the abnormal aggregation of mitochondria undergo cell death (39), HBx-expressing ChangX-31 and ChangX-34 cells have been maintained for years and did not show any apparent apoptotic characteristics by trypan blue exclusion assays and fluorescence-activated cell sorter analysis (data not shown). Expression of the HBx protein in these cells was confirmed by Western blot analysis (Fig. 1C). When subcellular localization of the HBx protein in HBx-expressing cells was determined by immunofluorescence staining using rabbit anti-HBx antibody, we found that HBx was localized in both the nucleus and the cytoplasm (Fig. 2A). Consistently, apparent perinuclear localization of mitochondria was reproducibly observed.

Organelles move along the cytoskeleton using microtubules for long-distance travel and actin for transport over short distances (43). Microtubules radiate from a microtubule organiz-

ing center (MTOC), which comprises a pair of centrioles and the surrounding pericentriolar material and is responsible for directing the polarity and orientation of microtubules during interphase (30). Previously, it was suggested that perinuclear localization of the HBx protein might be associated with the cytoskeleton (35). In fact, a close examination of mitochondrial aggregation at the nuclear periphery in HBx-expressing cells revealed an empty spot intensively surrounded by mitochondria (Fig. 2B, middle). Staining with an antibody against pericentrin, one of the major components of the pericentriolar materials, revealed that the HBx-associated mitochondrial aggregation was concentrated in the vicinity of the MTOC (Fig. 2B). These findings suggest that mitochondrial clustering could be associated with microtubules.

To examine this hypothesis, we used a microtubule-destabilizing drug (nocodazole) to test whether microtubules play an important role in organelle redistribution following HBx expression. We first determined the nocodazole concentration capable of depolymerizing microtubules under our treatment conditions and found that the treatment of Chang and ChangX-34 cells with 3.3 μM of nocodazole for 2 h resulted in a loss of microtubule filaments (fuzzy α-tubulin staining) (Fig. 2C, parts b and e). Removal of nocodazole by several washes with serum-containing medium restored microtubule nucleation within 5 min (data not shown). We found that mitochondrial aggregation in HBx-expressing cells was completely abolished when microtubules were depolymerized by nocodazole treatment (Fig. 2C, parts c and e). Surprisingly, the mitochondria in ChangX-34 cells rapidly reaggregated within 60 min of nocodazole release (Fig. 2C, parts c and f), indicating that a strong motor activity is involved in the transport of mitochondria in these cells. Similar data were obtained reproducibly from five independent experiments. The mitochondrial clustering in ChangX-34 cells was very fast, starting in the first 30 min after nocodazole release and finishing within 60 min, reforming the crescent shape of mitochondrion clustering (see Fig. 6B). In contrast, the mitochondria remained spread within the cytoplasm of control Chang cells before and after nocodazole release (Fig. 2C, parts b and c). These results clearly demonstrate that mitochondrial clustering occurs in a microtubule-dependent manner.

We also examined whether the actin skeleton is involved in mitochondrial redistribution in HBx-expressing cells. Control cells showed clear β-actin staining at the focal adhesions of the plasma membrane (Fig. 2D, parts a and d), while the addition of an actin polymerization inhibitor (cytochalasin D; 1 μM) for 1 h completely abrogated the actin cytoskeleton (Fig. 2D, parts b and e). The mitochondria in ChangX-34 cells remained aggregated (Fig. 2D, part e), even in the presence of cytochalasin D, indicating that the actin skeleton is not functionally involved in HBx-induced mitochondrial clustering. Thus, our results collectively demonstrated that the microtubule cytoskeleton, but not the actin skeleton, is indispensable for HBx-induced mitochondrial clustering. Our results also indicate that a system of active intracellular transport toward the nucleus must be involved in trafficking the mitochondria to the nuclear periphery.

Microtubule-dependent mitochondrial clustering occurs in HBV-replicating Huh7 cells. The abnormal mitochondrial aggregation was previously reported to occur only when high levels of the HBx protein were expressed (16). We employed HBV-related hepatoma cell lines in which HBx is expressed under the endogenous HBV promoter. SNU368 cells contain the HBV genome integrated into the chromosomes and express the HBx mRNA transcript (24), whereas Huh7 cells do not. Immunofluorescence staining against the HBx protein in SNU368 cells displayed HBx localized in the nucleus and cytoplasm (Fig. 3A), whereas no HBx protein was detected in Huh7 cells (Fig. 3A). Mitochondria in Huh7 cells homogeneously spread out through the cytoplasm, similar to those of Chang cells (Fig. 3A). On the contrary, the majority of SNU368 cells showed clustered mitochondria near the nucleus (Fig. 3A).

Next, we generated the Huh7-HBV cell lines by stably transfecting the HBV genome into Huh7 cells. The replication of the HBV genome in Huh7-HBV cells was determined by Southern blot analysis in which replicating HBV DNA was detected as single-stranded, double-stranded linear, and partially double-stranded relaxed circular HBV DNA (Fig. 3B). The 3.5-kb pregenomic RNA and 2.1- and 2.4-kb mRNA sequences of surface proteins with a fuzzy, smaller mRNA transcript were also detected in Huh7-HBV cells by Northern blot analysis (data not shown). In parental Huh7 cells, mitochondrial staining was scattered throughout the cytoplasm, whereas a dense ring-shaped mitochondrial staining surrounding the nuclear membrane was observed in Huh7-HBV cells (Fig. 3C, right). Typically, the area occupied by mitochondria in a cell was 30 to 50% in these cells, indicating that mitochondrial clustering can be induced under the endogenous level of HBx during HBV replication. Using a transient transfection system of the HBV replicon, we were also able to observe the abnormal mitochondrial morphology in a cells expressing HBx, whereas the nontransfected neighboring cell showed normal mitochondrial distribution (Fig. 3D, left and middle). However, in the transient transfection system, the abnormal mitochondrial morphology was induced only when high concentrations of the HBV replicon were expressed (data not shown), and clustered mitochondria were not as severe as those of cells stably expressing HBx or the HBV genome. In these cells, HBx was found mainly in the nucleus, but a weak cytoplasmic staining was also found (Fig. 3D, left). The HBx-dependent mitochondrial clustering in the HBV-replicating system was further confirmed in cells transfected with the HBx-negative HBV genome (pHBVX$^-$) in which mitochondrial clustering was no longer induced (Fig. 3D, right). In HBV-Huh7 cells, we again observed scattered mitochondria through the cytoplasm upon nocodazole treatment (Fig. 3E) where mitochondria were stained with MitoTrackerRed (red) and microtubules and the nucleus were visualized with fluorescein isothiocyanate-conjugated antibody (green) and DAPI (blue), respectively. Upon the removal of nocodazole by several washings with PBS, the scattered mitochondria rapidly reaggregated to the nuclear periphery within 1 h (Fig. 3E). In contrast, mitochondria in Huh7 cells remained scattered within the cytoplasm after nocodazole release (Fig. 3E). This is the first indication that mitochondrial clustering is induced in HBV-replicating cells in a microtubule-dependent manner. In addition, our data suggest that a system of active intracellular transport toward the nucleus must be involved in tracking the mitochondria to the nuclear periphery.

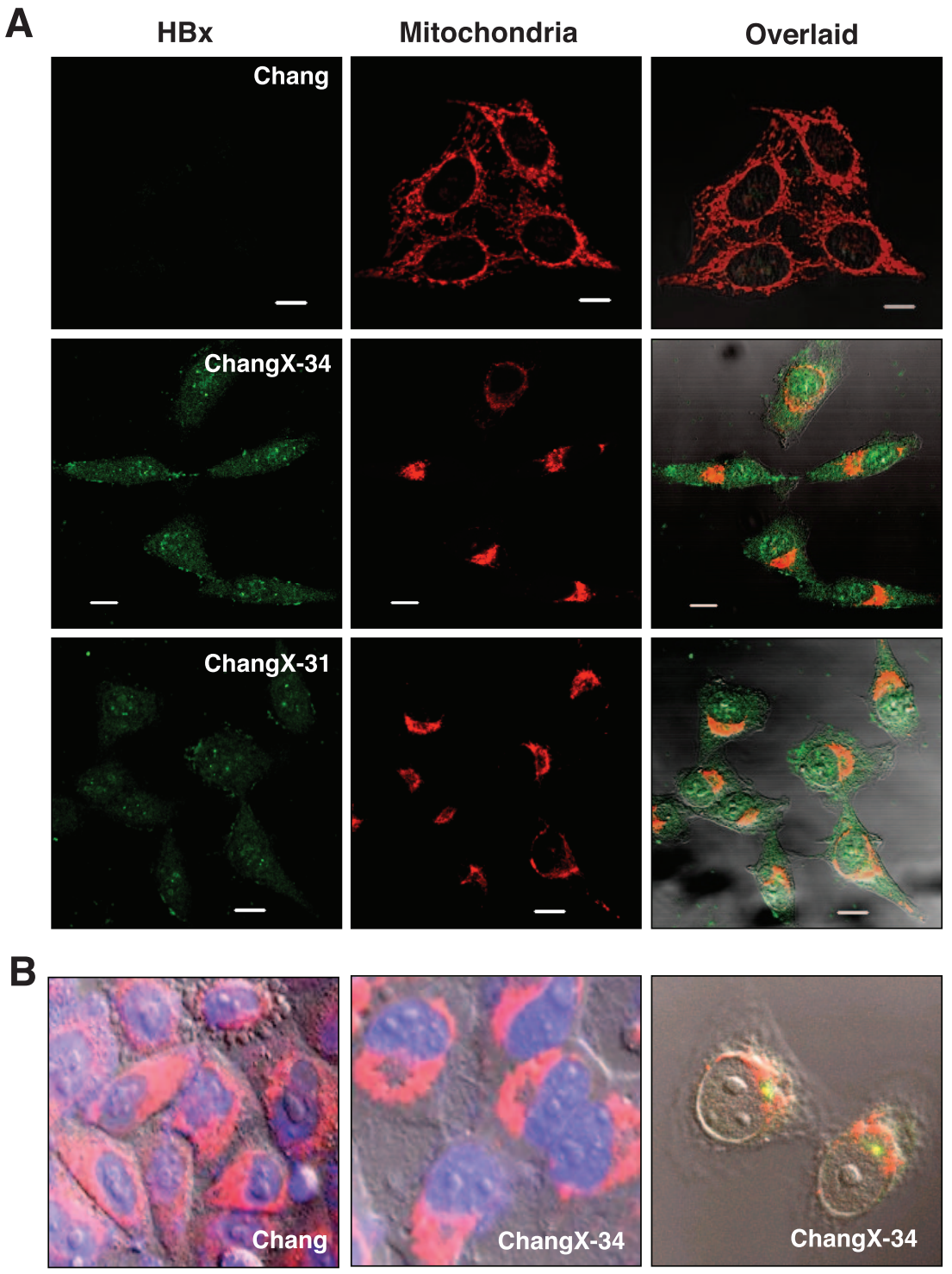

FIG. 2. Mitochondria migrate toward the MTOC in a microtubule-dependent manner in HBx-expressing cells. (A) Subcellular localizations of the HBx protein and mitochondria were visualized by immunofluorescence staining using anti-HBx antibody (green) and MitoTrackerRed (red) under a fluorescence microscope. The overlaid image was shown in the right panel, and the scale bar indicates 10 μm. (B) Chang and ChangX-34 cells were incubated with MitoTrackerRed for 30 min, and nuclei were subsequently stained with DAPI. The MTOC in ChangX-34 cells was identified by anti-pericentrin immunofluorescence (right panel). (C) Microtubules were depolymerized by the addition of 3.3 μM nocodazole (Noc) for 2 h and repolymerized by the removal of nocodazole by several washes with PBS. Mitochondria and α-tubulin (green) are representative of four independent experiments. (D) Actins were depolymerized by treatment with 1 μM cytochalasin D (Cyt. D) for 1 h and repolymerized by the removal of cytochalasin D. Mitochondria and β-actin (green) staining are representative of three different experiments. The crescent pattern of mitochondrion distribution was used as the criterion for judging mitochondrial clustering.

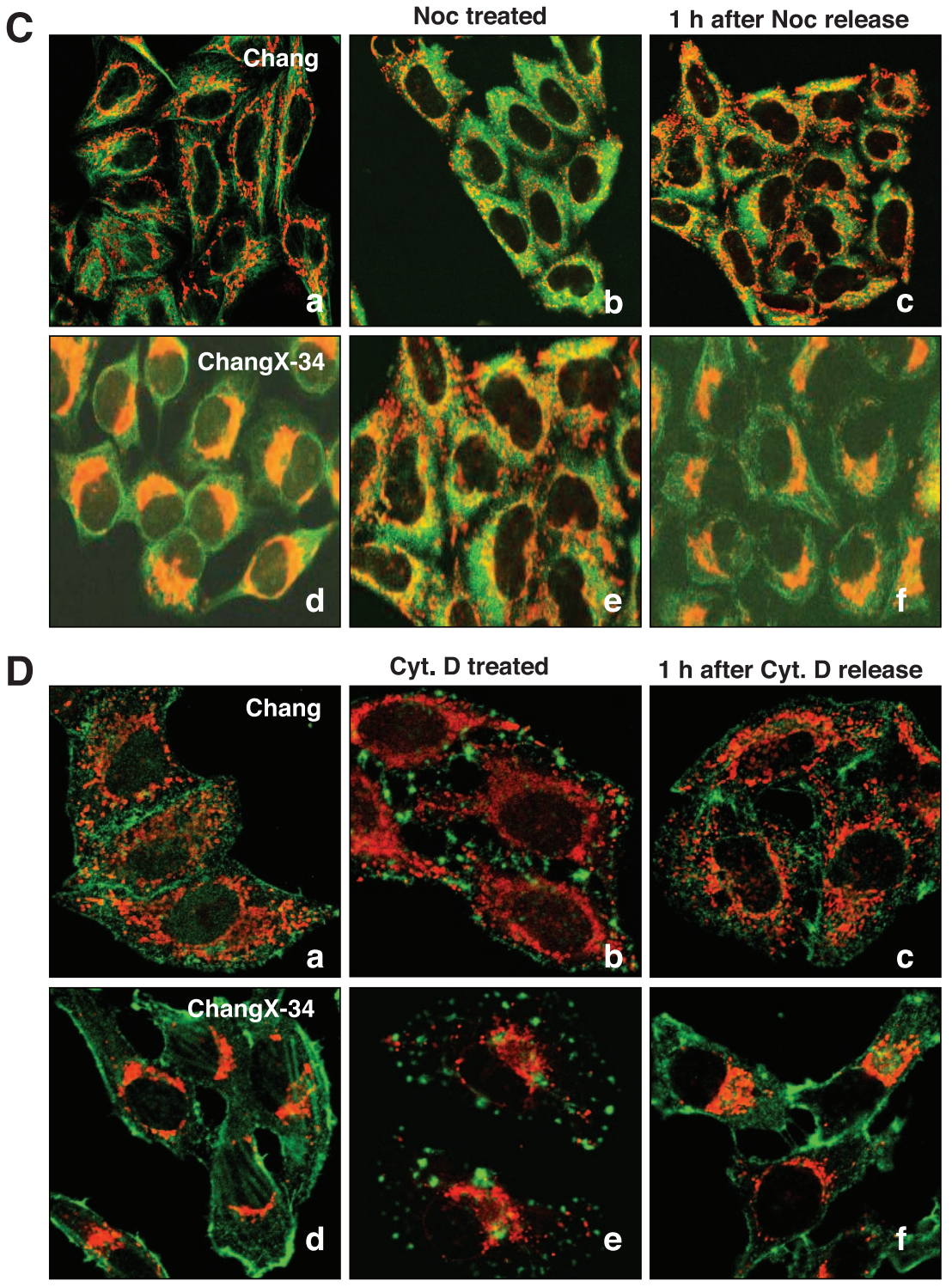

FIG. 2—*Continued.*

Inhibition of the dynein complex suppresses HBx-induced mitochondrial clustering. The microtubule-dependent transport of organelles occurs through the actions of two motor proteins, kinesin and dynein. Kinesin is mostly a plus-end-directed motor that moves toward the plasma membrane, whereas dynein is a minus-end-directed motor responsible for movement toward the nucleus or the MTOC. If dynein is involved in HBx-induced mitochondrial transport, we might expect the concentrated dynein complexes near the nucleus, where mitochondria are clustered. Dynein is a multisubunit complex composed of heavy, intermediate, light-intermediate, and light chains and includes the dynactin complex for motor activity. To detect the stable dynein complex attached to organelles or microtubules, soluble dynein was removed by per-

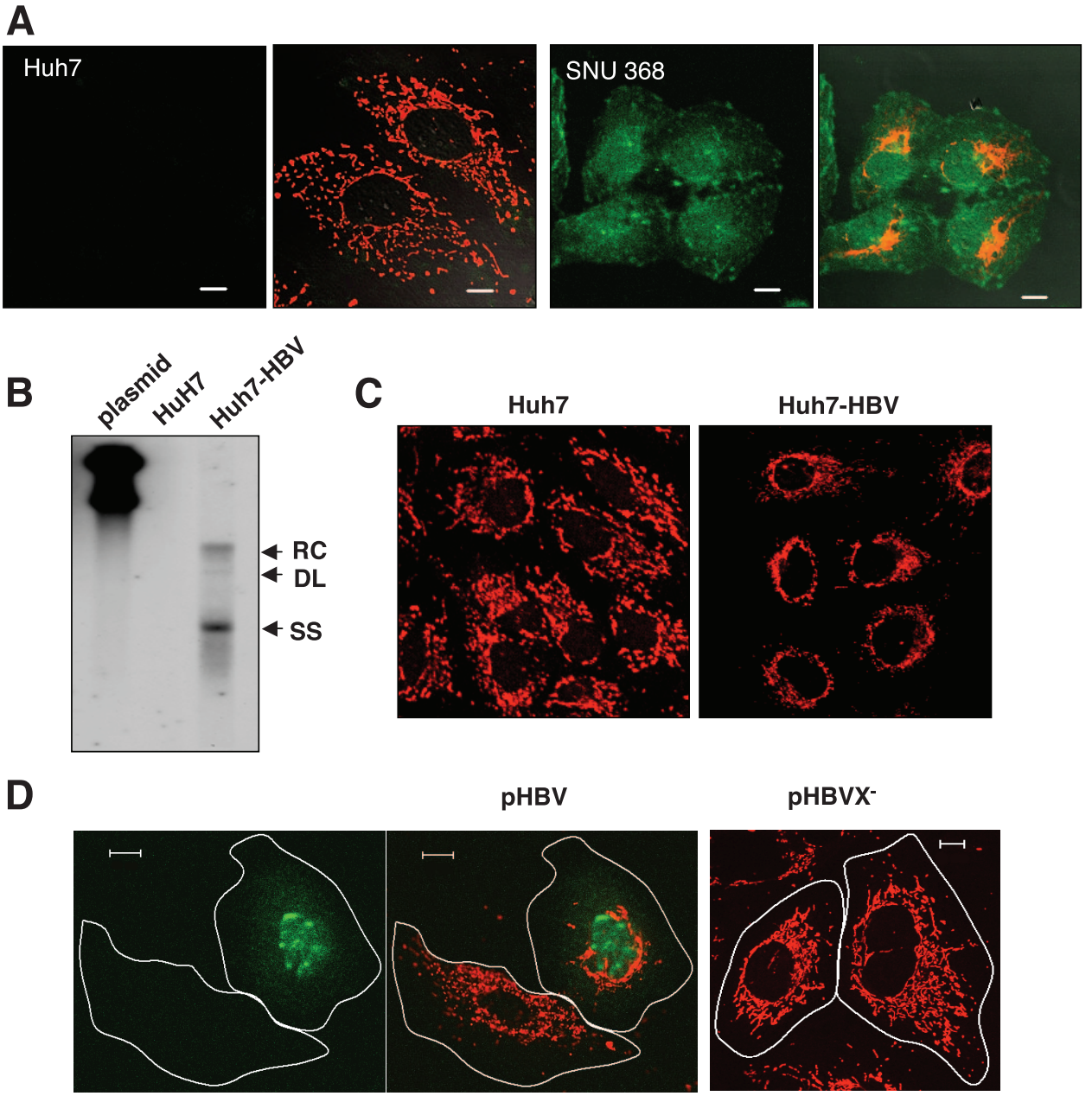

FIG. 3. Microtubule-dependent mitochondrial clustering occurs in HBV-replicating Huh7 cells. (A) Subcellular localizations of HBx and mitochondria in Huh7 and HBV-related SNU368 hepatoma cells were visualized by immunofluorescence staining using anti-HBx antibody (green) and MitoTrackerRed (red) under a fluorescence microscope. The scale bar indicates 10 μm. (B) HBV DNA was extracted from isolated core particles and analyzed by Southern blot analysis. Single- and double-stranded linear and partially double-stranded relaxed circular forms of HBV DNA are marked SS, DL, and RC, respectively. An HBV plasmid construct (1 ng) was used as a control marker. (C) Mitochondrial staining in Huh7 and HBV replicating Huh7-HBV cells. (D) Huh7 cells were transfected with a pHBV replicon (pHBV) or pHBV harboring a stop codon right after the AUG of the HBx gene (pHBVX$^-$) using the PEI method, and the subcellular localization of HBx (green) and mitochondria (red) was visualized by immunofluorescence staining. The scale bar indicates 10 μm. (E) Microtubules were depolymerized by the addition of 3.3 μM nocodazole (Noc) for 2 h and repolymerized by the removal of nocodazole by several washes with PBS. Mitochondria and α-tubulin were visualized by MitoTrackerRed and immunofluorescence staining. A representative image of three independent experiments is shown.

meabilizing cells with Triton X-100. When immunofluorescence staining against the DIC was carried out, we observed a spotty homogeneous distribution of DIC in Chang cells. On the other hand, the DIC staining in ChangX-34 cells was denser near the perinuclear region, where mitochondria were clustered (Fig. 4A). These were consistently observed in three separate experiments. Line scanning (from the plasma membrane to the nuclear periphery) demonstrated that the fluorescence intensity of DIC was relatively homogeneous through the cytoplasm of Chang cells, whereas it became stronger near the nuclear periphery of ChangX-31 or ChangX-34 cells. These results support our hypothesis that the dynein complex is involved in HBx-induced mitochondrial transport toward the MTOC.

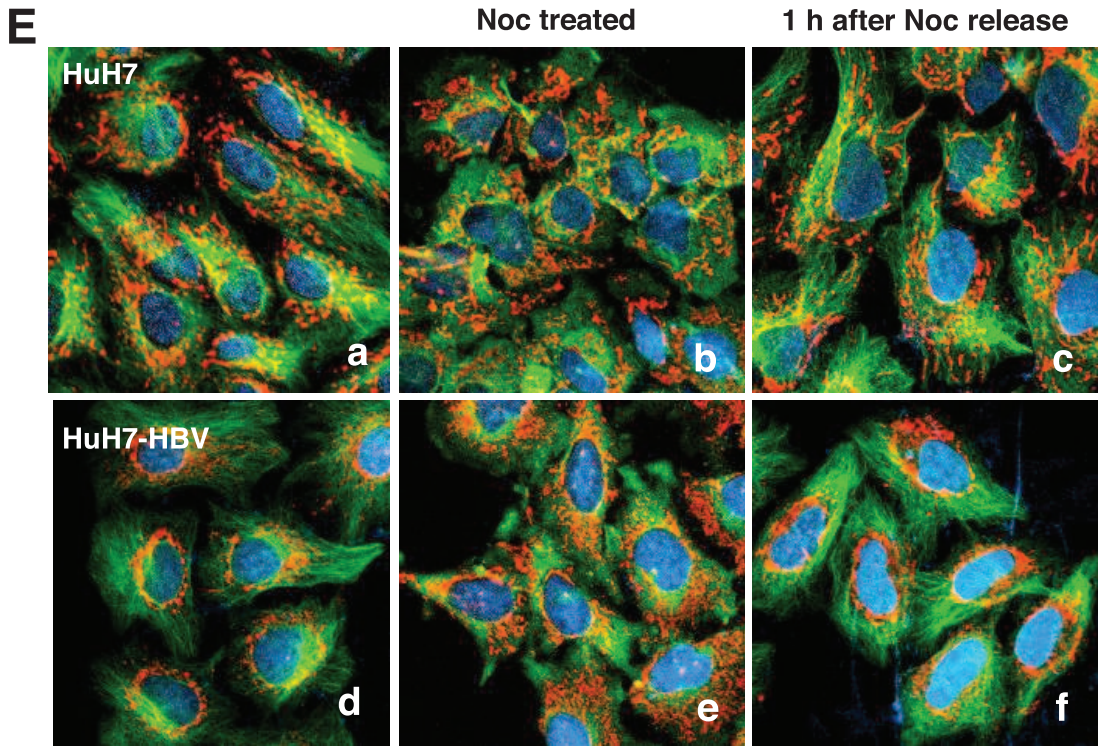

FIG. 3—*Continued.*

We next examined whether the inhibition of dynein activity in HBx-expressing cells could interfere with HBx-induced mitochondrial clustering. To test that, we used three different approaches. Dynamitin (p50) is one subunit of the dynactin complex, and overexpression of dynamitin in cells has been shown to disrupt dynein-dependent transport (7). We tested the role of dynein in HBx-induced mitochondrial clustering by transfecting cells with the pCMV-HBx expression vector alone or along with a dynamitin (p50) expression vector and determined the mitochondrial distribution after 48 h using parental Chang and Huh7 cells in which mitochondrial aggregation had been previously observed by HBx overexpression (39). Ectopic expression of pCMV-HBx along with pEGFP in Chang cells (Fig. 4B) and Huh7 cells (data not shown) induced the clustering of mitochondria. The area occupied by mitochondria in a cell was quantified using the LSM5 Image Browser according to the criteria described in Materials and Methods. The area occupied by mitochondria in control cells was determined to be 89% of the cytoplasmic area but was reduced to 53% upon HBx expression ($P < 0.001$, Student's t test). Coexpression of HBx and dynamitin, however, restored it back to the control level ($P < 0.001$, Student's t test). Thus, mitochondrial reclustering in HBx-expressing cells can be suppressed by the inhibition of dynein activity. We further tested whether the microinjection of HBx-expressing cells with a neutralizing antibody against dynein could reverse or suppress mitochondrial clustering. We carried out microinjection using either control IgG antibody or DIC-specific antibody with purified green fluorescent protein as an injection indicator (Fig. 4C). When the mitochondrial distribution patterns in ChangX-34 cells were examined 4 to 16 h after microinjection of the anti-DIC neutralizing antibody, we were not able to detect significant differences in the mitochondrial clustering pattern compared with uninjected ChangX-34 cells (data not shown). We interpreted these data to indicate that the inhibition of dynein activity is not effective enough to reverse mitochondrial clustering that had already occurred. Since mitochondrial reclustering was induced rapidly following nocodazole release in HBx-expressing cells (Fig. 2 and 3), we asked whether anti-dynein antibody can block/prevent reclustering following nocodazole treatment. We carried out the microinjection experiment under those experimental conditions. We incubated microinjected cells ($n = 300$) for 6 h, treated them with 100 ng/ml nocodazole for 2 h, and then washed the cells to remove the nocodazole. One hour after nocodazole release, the digital images of 50 to 100 mitochondria in each group were analyzed. Typically, the crescent pattern of mitochondrial reaggregation (mitochondrial area/cell of <60%) was observed in 83% of ChangX-34 cells injected with anti-IgG antibody (Fig. 4C, top), and 17% of cells didn't show clear clustering. Meanwhile, mitochondrial reclustering was suppressed in 72% of the cells injected with the DIC-specific antibody (Fig. 4C, white arrowheads), whereas neighboring noninjected ChangX-34 cells remained, displaying the crescent-shaped mitochondrial aggregates (Fig. 4C, yellow arrows). On average, the area of mitochondria per cell was increased to 85 to 90% when anti-DIC antibody was injected in two independent experiments. Finally, the treatment of ChangX-34 cells with 0.5 mM of EHNA, an inhibitor of dynein ATPase, almost completely suppressed the perinuclear reclustering of mitochondria (Fig. 4D and data not shown). Indeed, the reclustering of mitochondria was prominent upon nocodazole release, whereas mitochondria at the tip of the plasma membrane remained after EHNA treatment (data not shown). Collectively, these results indicate that

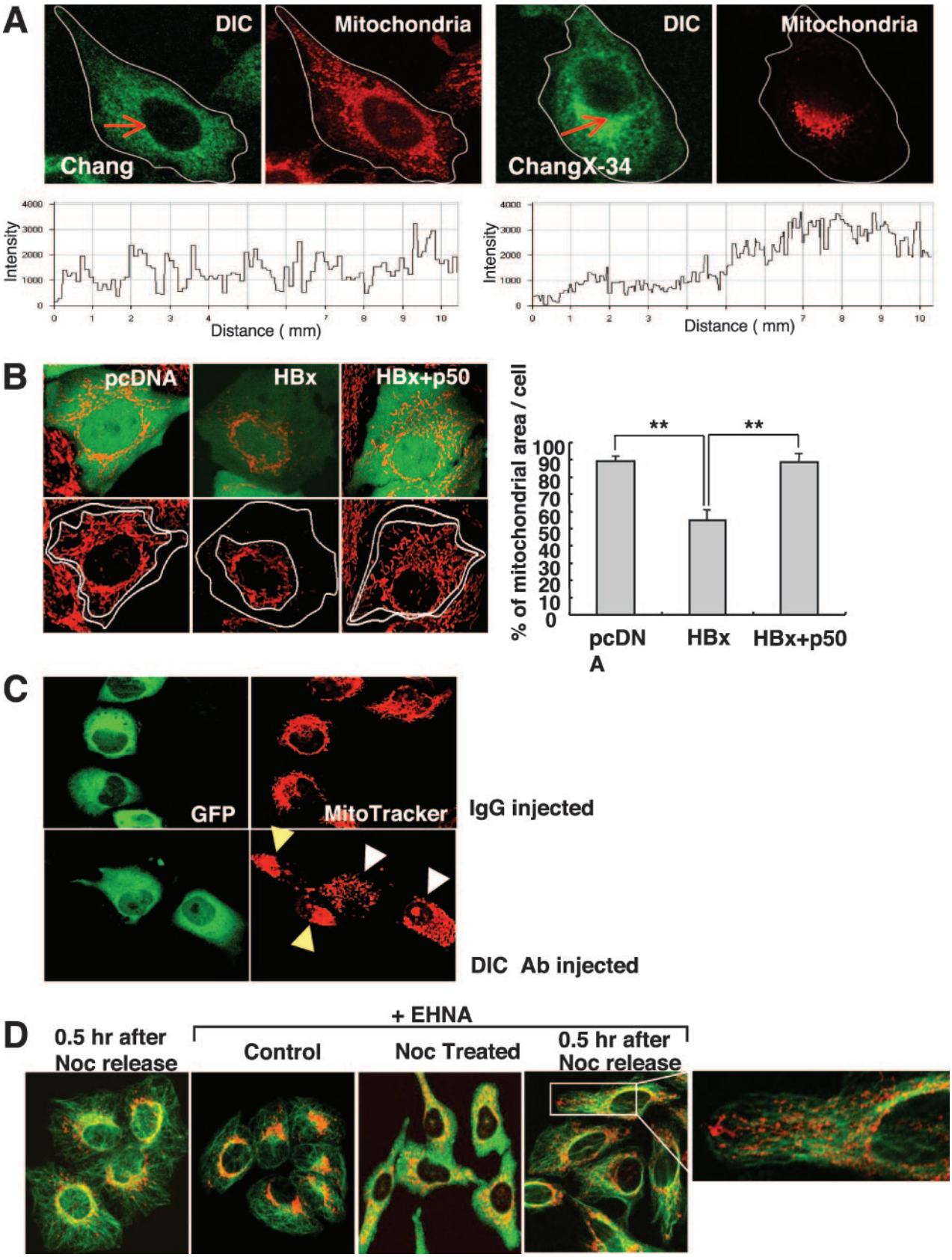
A
DIC
Mitochondria
Chang
DIC
Mitochondria
ChangX-34
Intensity
Distance (mm)
Intensity
Distance (mm)
B
pcDNA
HBx
HBx+p50
% of mitochondrial area / cell
**
**
pcDN A
HBx
HBx+p50
C
GFP
MitoTracker
IgG injected
DIC Ab injected
D
0.5 hr after Noc release
+ EHNA
Control
Noc Treated
0.5 hr after Noc release

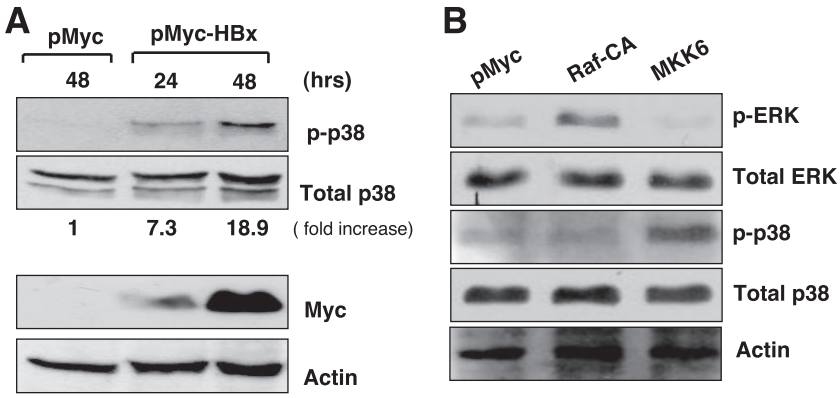

FIG. 5. HBx activates p38 MAPK. (A) Huh7 cells were transfected with the expression vector of HBx (pMyc-HBx) using PEI, and whole-cell lysates were obtained at 24 and 48 h after transfection. Expression levels of the phosphorylated form of p38 (p-p38), total p38, and HBx were determined by Western blotting and quantified using densitometry. The β-actin level indicates the normalization of protein levels in each lane. (B) Huh7 cells were transfected with the expression vector of pCDNA3 or Raf-CA or MKK6 expression vectors, and inductions of the phosphorylated ERK and p38 were determined by Western blotting at 24 h after transfection.

dynein motor activity is critically involved in HBx-induced mitochondrial clustering.

The p38 MAPK pathway mediates HBx-induced mitochondrial transport. Recent work has shown that the dynein-dependent motor activity can be modulated by the p38 MAPK (10). HBx has also been shown to stimulate many different signal transduction pathways in the cytoplasm, including the p38 MAPK pathways (40). We therefore attempted to determine whether the activation of the p38 MAPK by HBx can mediate mitochondrial clustering in our system. We found that the phosphorylated form of p38 was induced at 24 h upon HBx expression and became stronger at 48 h in Huh7 cells (Fig. 5A). Densitometric analysis revealed that the phosphorylated p38 level was increased by 7.3-fold at 24 h and 18.9-fold at 48 h compared to the total p38 protein level. Provided that the p38 MAPK pathway mediates the mitochondrial transport to the MTOC in our system, the overexpression of MKK6, encoding an upstream kinase of p38 MAPK, would be expected to mimic the mitochondrial clustering. We observed that the phosphorylated form of p38 was induced upon MKK6 overexpression (Fig. 5B). In contrast, the overexpression of Raf-CA, a constitutive active form of Raf, activated only the phosphorylated ERK and not the phosphorylated p38 in these cells. Next, we analyzed the MitoTrackerRed-stained cell images from cells expressing HBx, Raf-CA, or MKK6 along with the pEGFP expression vector in Huh7 cells using ImageArt software (Fig. 6A). The area occupied by mitochondria in a cell was calculated to be about 90% of the whole cytoplasmic area (Fig. 6A), whereas it was calculated to be ~50% ($P < 0.001$, Student's t test), in HBx- or MKK6-transfected Huh7 cells (Fig. 6A). On the other hand, Raf-CA overexpression did not alter the mitochondrial distribution in Huh7 cells (Fig. 6A). Thus, our results indicate that the activation of the p38 MAPK by HBx may be involved in mitochondrial transport to the MTOC.

Finally, we utilized several different signaling inhibitors to test the involvement of other signaling pathways in HBx-induced mitochondrial clustering. SB203580 (0.5 μM) (inhibitor of p38 MAPK), wortmannin (0.2 μM) (inhibitor of phosphoinositide 3-kinase), and calphostin C (0.25 μM) (inhibitor of protein kinase C) were separately applied to ChangX-34 cells ($n = 300$) right after nocodazole release, and mitochondrial reclustering was examined at 30 and 60 min. Mitochondrial clustering was seen in 80 to 90% of ChangX-34 cells prior to nocodazole treatment, which led to mitochondrial dispersal throughout the cytoplasm by nocodazole treatment (Fig. 6B and data not shown). At 30 min after nocodazole release, mitochondrial aggregation was found in about 70% of control ChangX-34 cells that did not receive any inhibitor treatment. Interestingly, the inhibition of the p38 MAPK pathway by treatment with 0.5 μM SB203580 significantly suppressed the reclustering of mitochondria in ChangX-34 cells ($P < 0.001$, Student's t test). Only 31% showed reclustering in ChangX-34

FIG. 4. Perinuclear clustering of mitochondria occurs in a dynein-dependent manner. (A) Cells were stained with MitoTrackerRed and permeabilized with 0.075% Triton X-100 in PHEM before fixation, and the distribution of the DIC was determined. The fluorescence image was acquired after Z-stack scanning. The arrows indicate line scanning (10 μm) starting from the side of the plasma membrane. The lower panel shows the corresponding scanning data. Representative data from three independent experiments are shown. (B) Chang cells were cotransfected with pCDNA3 (control), pMyc-HBx, and/or p50 (dynamitin) expression vectors along with plasmid pEGFP for the identification of transfected cells. The area occupied by mitochondria was quantified according to criteria described in Materials and Methods. Data shown on the right are the means ± standard deviations from two to four separate experiments (**$P < 0.001$ by Student's t test). (C) A neutralizing antibody (Ab) against DIC or control mouse IgG mixed with green fluorescent protein (GFP) was microinjected into cells ($n = 300$) using an automatic micromanipulator. Four hours later, cells were treated with 3.3 μM nocodazole for 2 h, washed, and examined for the subcellular localization of the mitochondria using confocal microscopy. White arrowheads indicate cells microinjected with the anti-DIC antibody, and yellow arrows represent neighboring noninjected ChangX-34 cells with clustered mitochondria. Two separate experiments were carried out. (D) ChangX-34 cells were pretreated with 0.5 mM EHNA for 0.5 h, which was followed by the addition of 3.3 μM nocodazole (Noc) for 2 h. Microtubules were repolymerized by the removal of nocodazole, and 0.5 mM EHNA was resupplied for 0.5 h. Mitochondria and α-tubulin (green) were visualized.

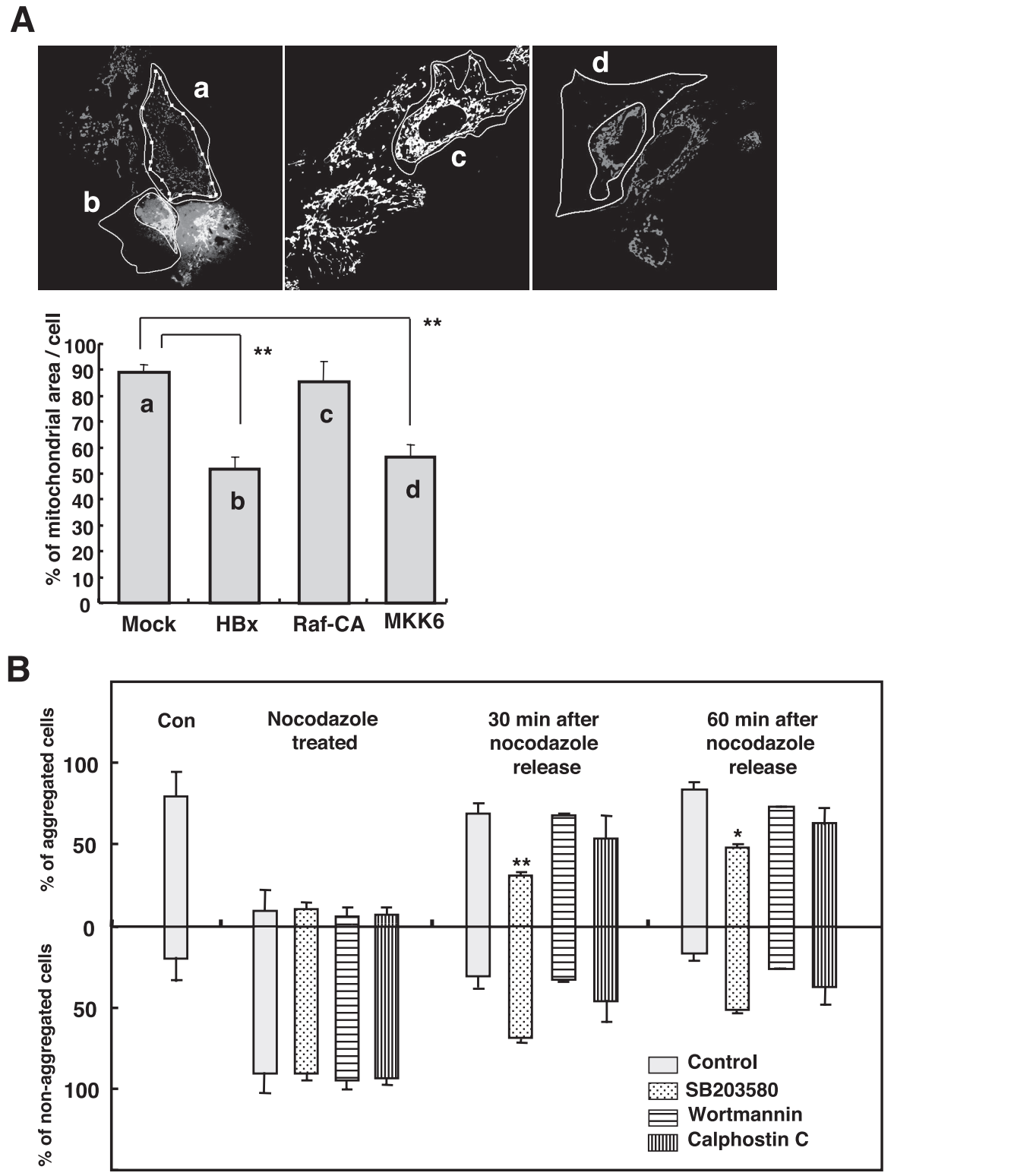

FIG. 6. Activation of p38 MAPK mediates mitochondrial clustering induced by HBx. (A) Huh7 cells were transfected with the expression vectors of HBx, Raf-CA, or MKK6 along with pEGFP, and the images of MitoTrackerRed-stained cell were obtained after 48 h. The area occupied by mitochondria in a cell was determined according to the criteria described in Materials and Methods. Data shown on the right are the means ± standard deviations from three independent experiments (**$P < 0.001$ by Student's t test). (B) The specific inhibitor SB203580 (0.5 μM), wortmannin (0.2 μM), or calphostin C (0.25 μM) was applied to ChangX-34 cells right after nocodazole release, and mitochondrial reclustering was examined at 30 and 60 min by MitoTrackerRed staining (data not shown). When the percentage of mitochondrial area per cell was <60%, it was considered to be aggregated cells, and those with >75% were considered to be nonaggregated cells. The bar represents means ± standard deviations from three separate experiments (*$P < 0.01$ and **$P < 0.001$ by Student's t test). Con, control.

cells (Fig. 6B) and ChangX-31 cells (data not shown), whereas none of the other signaling inhibitors exerted significant effects on mitochondrial reclustering in these cells. Higher concentrations of signaling inhibitors, up to 1 to 5 μM, yielded results similar to those shown in Fig. 6B (data not shown). At 60 min after nocodazole release, the reclustering of mitochondria in control ChangX-34 cells reached up to 84%, while only 48% of cells treated with SB203580 exhibited mitochondrial reclustering ($P < 0.01$, Student's t test). At this time point, 73% of wortmannin-treated ChangX-34 cells showed mitochondrial aggregation, as did 63% of calphostin C-treated ChangX-34 cells. Thus, our results indicate that the p38 MAPK in HBx-expressing cells is actively, but not exclusively, involved in mitochondrial transport to the MTOC. Collectively, these results indicate that the activation of p38 MAPK by HBx plays a critical role in the alteration of intracellular motility, resulting in mitochondrial clustering.

DISCUSSION

The data reported here show a novel HBx function in the regulation of intracellular motility. We showed that HBx activation of the p38 MAPK contributed to the increase in the microtubule-dependent dynein activity, which is attributed to mitochondrial aggregation.

Initially, mitochondrial aggregation by HBx was found in cells undergoing cell death. It is believed that cells expressing high levels of HBx were prone to apoptosis (22, 35, 39), and high levels of HBx expression, but not moderate or low levels of HBx, were shown to induce abnormal mitochondrion distribution (16). In our experimental systems, however, ChangX-31 and ChangX-34 sublines express moderate levels of HBx. In these cells, HBx was transcribed from the Tet-on promoter without doxycycline stimulus (45, 46). Moreover, the HBx level in HBV-Huh7 cells is controlled by the endogenous HBV promoter and was beyond the limit of detection by Western blotting. In both cases, apparent mitochondrial clustering was induced, indicating that mitochondrial aggregation can be induced under moderate or low physiological levels of HBx. These results differ from those of the a previous report by Henkler et al. (16), which can be partly explained by the experimental systems. Those authors used only transient transfection systems in which they observed cells for short periods. Using the transient transfection system, we observed perinuclear aggregation of mitochondria, but the extent was weaker. Collectively, the mitochondrial clustering at the nuclear periphery was not limited to the cells that were constructed to express high levels of HBx but can occur broadly in HBV-related liver cells during chronic viral infection. Moreover, mitochondrial aggregation in liver cells may represent a cellular process that underlies the pathogenic disease progression during chronic viral infection.

We have further demonstrated that mitochondrial clustering occurs in a microtubule-dependent manner and that HBx modulates the microtubule-dependent dynein activity. First, the dynein concentration was high at the nuclear periphery where mitochondria aggregated. Second, HBx-induced perinuclear mitochondrial clustering was inhibited by the coexpression of HBx and dynamitin, which disrupts the proper assembly of the dynein complex (7). Third, microinjection of a neutralizing anti-DIC antibody suppressed the reclustering of mitochondria in HBx-expressing cells. Finally, the inhibition of dynein ATPase activity by EHNA almost completely prevents mitochondrial reclustering. All our results collectively indicate that the dynein minus-end motor likely plays an active role in transporting mitochondria toward the MTOC in HBx-expressing cells. Theoretically, however, perinuclear mitochondrial clustering could occur through either strong minus-end motor activity or weak plus-end motor activity. At present, our experiments do not allow us to completely exclude the possibility that kinesin-dependent plus-end motor activity is somehow involved in mitochondrial clustering in HBx-expressing cells.

So far, the role of the intracellular transport machinery during HBV replication has never been studied, and to our knowledge, the data here are the first indication that HBx is capable of modulating intracellular motility. During HBV infection, HBV enters hepatocytes by endocytosis, and the nucleocapsid must enter the nucleus for the establishment of viral replication. Progeny HBV particles are assembled in the cytosol and can be released out of hepatocytes or are thought to reenter to the nucleus for another cycle of viral replication. It seems logical that the microtubule cytoskeleton can be tightly associated with HBV pathogenesis. Given the HBx function in the microtubule-dependent dynein activity, HBx may also modulate intracellular transport and the assembly of progeny particles. This can be supported by other viral pathogens of adenovirus for which nuclear targeting was affected by microtubule-dependent intracellular motilities (38). In addition, different kinds of viral proteins such as HSV-1 nuclear and capsid proteins or retroviral Gag protein directly interacted with dynein (13, 31) or kinesin (1).

Whether the mitochondrion-associated HBx mediates the intracellular motility remains to be analyzed. We have shown that the dynein-dependent motor activity causing mitochondrial reaggregation is mediated by p38 MAPK activity. HBx was shown to interact directly with the mitochondrial protein VDAC3, and HBx itself also seemed to contain a transmembrane region that targets the mitochondrial membrane (19, 33). HBx at the mitochondria most affected the mitochondrial dysfunction by lowering the mitochondrial membrane potential and elevating the ROS level (33, 35, 39, 42). It is possible that the p38 MAPK can be activated downstream of the elevated ROS (18) initiated by the mitochondrion-associated HBx. Alternatively, the activation of the p38 MAPK in general can be mediated by the upstream cytoplasmic signaling cascades (14, 15). HBx was shown to induce multiple cytoplasmic signaling pathways (5, 8, 12, 23, 26), and therefore, cytoplasmic HBx may stimulate the upstream signaling activators of p38 MAPK. It is of note that calcium signaling is important in microtubule organization and vesicle transport (44), and cytosolic calcium can be mobilized by HBx (4, 5). Therefore, together, our data raise a possibility that both calcium signaling and the p38 MAPK activated by HBx may cooperate to regulate the efficiency of movement of the subviral HBV particles.

In summary, we herein demonstrated that (i) HBx induces perinuclear clustering of mitochondria in a microtubule-dependent manner and (ii) functional blockage of dynein and p38 MAPK suppressed mitochondrial movement. These data suggest that HBx plays a novel regulatory role in subcellular transport systems, perhaps facilitating the process of maturation

and/or assembly of progeny particles during HBV replication. Furthermore, mitochondrial aggregation induced by HBx may represent a cellular process that underlies disease progression during chronic viral infection.

ACKNOWLEDGMENTS

We greatly appreciate Wang-Shick Ryu (Yonsei University, Korea) for his critical comments on the manuscript.

This study was supported by grants of the Korea Research Foundation (KRF EP0030) and partly by the Korea Science and Engineering Foundation through the Chronic Inflammatory Disease Research Center (R13-2003-019), Republic of Korea. S. Kim and S. Lee are supported by the BK21 program, Korean Ministry of Education.

REFERENCES

1. **Benboudjema, L., M. Mulvey, Y. Gao, S. W. Pimplikar, and I. Mohr.** 2003. Association of the herpes simplex virus type 1 Us11 gene product with the cellular kinesin light-chain-related protein PAT1 results in the redistribution of both polypeptides. J. Virol. **77:**9192–9203.
2. **Blum, H. E., E. Galun, T. J. Liang, F. von Weizsacker, and J. R. Wands.** 1991. Naturally occurring missense mutation in the polymerase gene terminating hepatitis B virus replication. J. Virol. **65:**1836–1842.
3. **Bouchard, M. J., and R. J. Schneider.** 2004. The enigmatic X gene of hepatitis B virus. J. Virol. **78:**12725–12734.
4. **Bouchard, M. J., L. H Wang, and R. J. Schneider.** 2001. Calcium signaling by HBx protein in hepatitis B virus DNA replication. Science **294:**2376–2378.
5. **Bouchard, M. J., R. J. Puro, L. Wang, and R. J. Schneider.** 2003. Activation and inhibition of cellular calcium and tyrosine kinase signaling pathways identify targets of the HBx protein involved in hepatitis B virus replication. J. Virol. **77:**7713–7719.
6. **Brechot, C.** 2004. Pathogenesis of hepatitis B virus-related hepatocellular carcinoma: old and new paradigms. Gastroenterology **127:**S56–S61.
7. **Burkhardt, J. K., C. J. Echeverri, T. Nilsson, and R. G. Vallee.** 1997. Overexpression of the dynamitin (p50) subunit of the dynactin complex disrupts dynein-dependent maintenance of membrane organelle distribution. J. Cell Biol. **139:**469–484.
8. **Cha, M. Y., C. M. Kim, Y. M. Park, and W. S. Ryu.** 2004. Hepatitis B virus X protein is essential for the activation of Wnt/beta-catenin signaling in hepatoma cells. Hepatology **39:**1683–1693.
9. **Cheong, J. H., M. Yi, Y. Lin, and S. Murakami.** 1995. Human RPB5, a subunit shared by eukaryotic nuclear RNA polymerases, binds human hepatitis B virus X protein and may play a role in X transactivation. EMBO J. **14:**143–150.
10. **Cheung, P. Y., Y. Zhang, J. Long, S. Lin, M. Zhang, Y. Jiang and Z. Wu.** 2004. p150 (Glued), dynein, and microtubules are specifically required for activation of MKK3/6 and p38 MAPKs. J. Biol. Chem. **279:**45308–45311.
11. **Dandri, M., P. Schirmacher, and C. E. Rogler.** 1996. Woodchuck hepatitis virus X protein is present in chronically infected woodchuck liver and woodchuck hepatocellular carcinomas which are permissive for viral replication. J. Virol. **70:**5246–5254.
12. **Doria, M., N. Klein, R. Lucito, and R. J. Schneider.** 1995. The hepatitis B virus HBx protein is a dual specificity cytoplasmic activator of Ras and nuclear activators of transcription factors. EMBO J. **14:**4747–4757.
13. **Douglas, M. W., R. J. Diefenbach, F. L. Homa, M. Miranda-Saksena, F. J. Rixon, V. Vittone, K. Byth, and A. L. Cunningham.** 2004. Herpes simplex virus type 1 capsid protein VP26 interacts with dynein light chains RP3 and Tctex1 and plays a role in retrograde cellular transport. J. Biol. Chem. **279:**28522–28530.
14. **Ellinger-Ziegelbauer, H., K. Brown, K. Kelly, and U. Siebenlist.** 1997. Direct activation of the stress-activated protein kinase (SAPK) and extracellular signal-regulated protein kinase (ERK) pathways by an inducible mitogen-activated protein kinase/ERK kinase kinase 3 (MEKK) derivative. J. Biol. Chem. **272:**2668–26674.
15. **Hagemann, C., and J. L. Blank.** 2001. The ups and downs of MEK kinase interactions. Cell. Signal. **13:**863–875.
16. **Henkler, F., J. Hoare, N. Waseem, R. D. Goldin, M. J. McGarvey, R. Koshy, and I. A. King.** 2001. Intracellular localization of the hepatitis B virus HBx protein. J. Gen. Virol. **82:**871–882.
17. **Hoare, J., F. Henkler, J. J. Dowling, W. Errington, R. D. Goldin, D. Fish, and M. J. McGarvey.** 2001. Subcellular localisation of the X protein in HBV infected hepatocytes. J. Med. Virol. **64:**419–426.
18. **Hsieh, C. C., and J. Papaconstantinou.** 2006. Thioredoxin-ASK1 complex levels regulate ROS-mediated p38 MAPK pathway activity in livers of aged and long-lived Snell dwarf mice. FASEB J. **20:**259–268.
19. **Huh, K. W., and A. Siddiqui.** 2002. Characterization of the mitochondrial association of hepatitis B virus X protein, HBx. Mitochondrion **1:**349–359.
20. **Jin, Y. M., C. Yun, C. Park, H. J. Wang, and H. Cho.** 2001. Expression of hepatitis B virus X protein is closely correlated with the high periportal inflammatory activity of liver diseases. J. Viral Hepat. **8:**322–330.
21. **Kim, H. Y., G. S. Park, E. G. Kim, S. H. Kang, H. J. Shin, S. Park, and K. M. Kim.** 2004. Oligomer synthesis by priming deficient polymerase in hepatitis B virus core particle. Virology **322:**22–30.
22. **Kim, Y. C., K. S. Song, G. Yoon, M. J. Nam, and W. S. Ryu.** 2001. Activated ras oncogene collaborates with HBx gene of hepatitis B virus to transform cells by suppressing HBx-mediated apoptosis. Oncogene **20:**16–23.
23. **Klein, N. P., and R. J. Schneider.** 1997. Activation of Src family kinases by hepatitis B virus HBx protein and coupled signaling to Ras. Mol. Cell. Biol. **17:**6427–6436.
24. **Lee, J. H., J. L. Ku, Y. J. Park, K. J. U. Lee, W. H. Kim, and J. G. Park.** 1999. Establishment and characterization of four human hepatocellular carcinoma cell lines containing hepatitis B virus DNA. World J. Gastroenterol. **5:**289–295.
25. **Lee, Y. I., J. M. Hwang, J. H. Im, Y. I. Lee, N. S. Kim, D. G. Kim, D. Y. Yu, H. B. Moon, and S. K. Park.** 2004. Human hepatitis B virus-X protein alters mitochondrial function and physiology in human liver cells. J. Biol. Chem. **279:**15460–15471.
26. **Lee, Y. I., S. Kang-Park, S. I. Do, and Y. I. Lee.** 2001. The hepatitis B virus-X protein activates a phosphatidylinositol 3-kinase-dependent survival signaling cascade. J. Biol. Chem. **276:**16969–16977.
27. **Lin, Y., T. Nomura, J. Cheong, D. Dorjsuren, K. Iida, and S. Murakami.** 1997. Hepatitis B virus X protein is a transcriptional modulator that communicates with transcription factor IIB and the RNA polymerase II subunit 5. J. Biol. Chem. **272:**7132–7139.
28. **Maguire, H. F., J. P. Hoeffler, and A. Siddiqui.** 1991. HBV X protein alters the DNA binding specificity of CREB and ATF-2 by protein-protein interactions. Science **252:**842–844.
29. **Margolis, H. S., M. J. Alter, and S. C. Hadler.** 1991. Hepatitis B: evolving epidemiology and implications for control. Semin. Liver Dis. **11:**84–92.
30. **Megraw, T. L., S. Kilaru, F. R. Turner, and T. C. Kaufman.** 2002. The centrosome is a dynamic structure that ejects PCM flares. J. Cell Sci. **115:**4707–4718.
31. **Petit, C., M. L. Giron, J. Tobaly-Tapiero, P. Bittoun, E. Real, Y. Jacob, N. Tordo, H. De The, and A. Saib.** 2003. Targeting of incoming retroviral Gag to the centrosome involves a direct interaction with the dynein light chain 8. J. Cell Sci. **116:**3433–3442.
32. **Qadri, I., J. W. Conaway, R. C. Conaway, J. Schaack, and A. Siddiqui.** 1996. Hepatitis B virus transactivator protein, HBx, associates with the components of TFIIH and stimulates the DNA helicase activity of TFIIH. Proc. Natl. Acad. Sci. USA **93:**10578–10583.
33. **Rahmani, Z., K. W. Huh, R. Lasher, and A. Siddiqui.** 2000. Hepatitis B virus X protein colocalizes to mitochondria with a human voltage-dependent anion channel, HVDAC3, and alters its transmembrane potential. J. Virol. **74:**2840–2846.
34. **Ryu, W. S.** 2003. Molecular aspects of hepatitis B viral infection and the viral carcinogenesis. J. Biochem. Mol. Biol. **36:**138–143.
35. **Shirakata, Y., and K. Koike.** 2003. Hepatitis B virus X protein induces cell death by causing loss of mitochondrial membrane potential. J. Biol. Chem. **278:**22071–22078.
36. Reference deleted.
37. **Spandau, D. F., and C.-H. Lee.** 1988. *trans*-activation of viral enhancers by the hepatitis B virus X protein. J. Virol. **62:**427–434.
38. **Suomalainen, M., M. Y. Nakano, S. Keller, K. Boucke, R. P. Stidwill, and U. F. Greber.** 1999. Microtubule-dependent plus- and minus end-directed motilities are competing processes for nuclear targeting of adenovirus. J. Cell Biol. **144:**657–672.
39. **Takada, S., Y. Shirakata, N. Kaneniwa, and K. Koike.** 1999. Association of hepatitis B virus X protein with mitochondria causes mitochondrial clustering at the nuclear periphery, leading to cell death. Oncogene **18:**6965–6973.
40. **Tarn, C., L. Zou, R. L. Hullinger, and O. M. Andrisani.** 2002. Hepatitis B virus X protein activates the p38 mitogen-activated protein kinase pathway in dedifferentiated hepatocytes. J. Virol. **76:**9763–9772.
41. **Twu, J. S., and R. H. Schloemer.** 1989. Transcription of the human beta interferon gene is inhibited by hepatitis B virus. J. Virol. **63:**3065–3071.
42. **Waris, G., K. W. Huh, and A. Siddiqui.** 2001. Mitochondrially associated hepatitis B virus X protein constitutively activates transcription factors STAT-3 and NF-kappa B via oxidative stress. Mol. Cell. Biol. **21:**7721–7730.
43. **Yaffe, M. P., D. Harata, F. Verde, M. Eddison, T. Toda, and P. Nurse.** 1996. Microtubules mediate mitochondrial distribution in fission yeast. Proc. Natl. Acad. Sci. USA **93:**11664–11668.
44. **Yi, M., D. Weaver, and G. Hajnoczky.** 2004. Control of mitochondrial motility and distribution by the calcium signal: a homeostatic circuit. J. Cell Biol. **167:**661–672.
45. **Yun, C., H. Cho, S. J. Kim, J. H. Lee, S. Y. Park, G. Chan, and H. Cho.** 2004. Mitotic aberration coupled with centrosome amplification is induced by hepatitis B virus X oncoprotein via the Ras-mitogen-activated protein/extracellular signal-regulated kinase-mitogen-activated protein pathway. Mol. Cancer Res. **2:**159–169.
46. **Yun, C., J. H. Lee, H. Park, Y. M. Jin, S. Park, K. Park, and H. Cho.** 2000. Chemotherapeutic drug, adriamycin, restores the function of p53 protein in hepatitis B virus X (HBx) protein-expressing liver cells. Oncogene **19:**5163–5172.